Effective Immobilization of Tyrosinase via Enzyme Catalytic Polymerization of l-DOPA for Highly Sensitive Phenol and Atrazine Sensing

Yun Guan, Lanjunzi Liu, Chao Chen, Xiuzhi Kang, Qingji Xie

www.elsevier.com/locate/talanta

PII: S0039-9140(16)30494-5
DOI: http://dx.doi.org/10.1016/j.talanta.2016.07.003
Reference: TAL16700

To appear in: *Talanta*

Received date: 9 March 2016
Revised date: 24 June 2016
Accepted date: 2 July 2016

Cite this article as: Yun Guan, Lanjunzi Liu, Chao Chen, Xiuzhi Kang and Qingj Xie, Effective Immobilization of Tyrosinase via Enzyme Catalyti Polymerization of l-DOPA for Highly Sensitive Phenol and Atrazine Sensing *Talanta,* http://dx.doi.org/10.1016/j.talanta.2016.07.003

Effective Immobilization of Tyrosinase via Enzyme Catalytic Polymerization of L-DOPA for Highly Sensitive Phenol and Atrazine Sensing

Yun Guan, Lanjunzi Liu, Chao Chen*, Xiuzhi Kang, Qingji Xie*

Key Laboratory of Chemical Biology and Traditional Chinese Medicine Research (Ministry of Education), College of Chemistry and Chemical Engineering, Hunan Normal University, Changsha 410081, PR China

chenchao840103@163.com (C. Chen)
xieqj@hunnu.edu.cn (Q. Xie).
*Corresponding author. Tel & Fax: +86-731-8865515.

ABSTRACT

The facile preparation of poly(L-DOPA)-tyrosinase (PD_M-Tyr) composite and its application both in substrate (phenol) and inhibitor (atrazine) sensing is reported here for the first time. Effective immobilization of enzyme is realized via in-situ entrapping Tyr in poly(L-DOPA) (PD_M), which is formed by Tyr catalytic polymerization of L-DOPA. The Tyr modified electrode is simply prepared by dipping the PD_M-Tyr composite on an Au electrode and then covered by Nafion. The thus-prepared Tyr-immobilized electrode exhibits excellent performance superior to most Tyr-based electrochemical biosensors, the sensitivity to phenol is as high as 5122 μA mM^{-1} in the linear range of 10 nM ~ 1.25 μM, the apparent Michaelis-Menten constant (K_M^{app}) determined as low as 3.13 μM indicates strong substrate binding and high catalytic activity of the immobilized Tyr. The biosensor also works well in atrazine biosensing, with a linear detection range of 50 ppb ~ 30 ppm and a low detection limit of 10 ppb obtained. In addition, the biosensor shows excellent stability, precision, high sensitivity and fabrication simplicity.

Keywords: L-DOPA, tyrosinase modified electrode, enzyme-catalyzed polymerization, phenolic compounds biosensing, atrazine biosensing.

1. Introduction

Tyrosinase (Tyr), also known as polyphenol oxidase, is a copper-containing enzyme that plays a crucial role in melanin biosynthesis and in enzymatic browning of fruits, vegetables, and crustaceans [1-2]. Tyr activity is an ideal indicative marker for the presence of cancerous growths because elevated amounts of Tyr can be detected in melanoma cancer cells [3]. The Tyr-catalytic oxidation of phenols has been widely applied to the biosensing of bisphenol A, phenol, catechol, dopamine, and etc. [4-12] In addition, the Tyr inhibition has also received great concern because of its wide application in preventing unfavorable darkening from enzymatic oxidation of phenols, in medicinal, and in cosmetic products in relation to hyperpigmentation [13]. The flavonols isolated from the crocus flower petals and their congeners were studied for their Tyr inhibitory activity. So the investigation on the enzymatic catalysis and enzyme inhibition of Tyr is of great significance.

Phenolic compounds widely existing in industrial wastewaters are causing many serious environmental problems. High levels of phenols have been demonstrated to be of detrimental effects on animal health and many phenols are listed as dangerous substances or priority pollutants by the European Commission (EC) and the United States Environmental Protection Agency (U.S.EPA).[14] Atrazine (2-chloro-4-ethylamino-6-isopropyl-amino-1,3,5-triazine) is one of the most widely used herbicides which may cause serious health risks even at very low levels (ppb level) [15]. Due to the large amount and the continuous use of atrazine as herbicide for many years, environmental problems causing by atrazine have become serious and apparent [16]. The long exposure of atrazine has been identified reproductive and can induce developmental abnormalities [17]. Therefore, developing novel analytical techniques for fast monitoring of environmental phenolic pollutants and atrazine is of great significance and highly required for increasing legislative and environmental control [18-19]. Conventional methods for phenols and atrazine determination mainly include gas or liquid chromatography and spectrophotometry [20-21]. However, their disadvantages such as time-consuming, demanding sample pretreatments,

requiring qualified and experienced staffs and inconvenience for on-site or in-field detection greatly limit their practical applications. Electrochemical biosensors are considered as an ideal candidate for detecting pollutants due to the advantages such as selectivity, simplicity, sensitivity, operational feasibility, and easy miniaturization [12, 22]. The oxidation of phenols to catechols and then to *o*-quinones is catalyzed by Tyr, the reduction current of *o*-quinones reduced back to catechols by the electrode can be detected at the electrode and used to indicate the presence of phenols. Meanwhile, when the enzymatic activity of Tyr is inhibited by atrazine, the reduction current will be lowered proportional to the concentration of the inhibitor, so the inhibition percentage can be used to quantify atrazine [23-24]. Various Tyr-based biosensors have thus been proposed for the determination of phenols and their derivatives, with atrazine biosensors based on Tyr inhibition widely reported [4, 24-26].

The immobilization of biomolecules plays an important role in bioscience and biotechnology. The high-load and high-activity immobilization of enzyme is a big concern in biocatalysis and biosensing fields [27]. Dopamine (DA), an important hormones and neurotransmitters with similar structure as L-DOPA, has been widely studied and used for membrane fabrication/modification [28-35] and enzyme immobilization [36-40] due to the adhesion ability and facile deposition process of its polymer. The polymers prepared by DA electrochemical oxidation (PDA_E)[41], DA chemical oxidation (PDA_C) [42-43], and DA enzymatic oxidation (PDA_M) [44] have been recognized as excellent biocompatible matrices to entrap biomacromolecules at high load/activity. Poly(L-DOPA) (PD) as an amino acid polymer has the higher biocompatibility and more favorable affinity to enzyme than dopamine (PDA), so it is expected to serve well as enzyme immobilization matrix. Many research reports have shown the versatile applications of L-DOPA relevant to its surface-adhesive characteristic [45-46]. Recently, our lab has reported the electrochemical/chemical oxidative synthesis and biosensing/biofuel cell applications of PD studied versus PDA as a recent hotspot biomaterial [47]. The enzyme-catalyzed polymerization of L-DOPA was also investigated to immobilize enzymes for

biosensing of H_2O_2, uric acid, catechol and glucose [48-49]. The enzyme electrode developed by coelectrodeposition of PD and enzyme shows biosensing performance superior to that of the corresponding enzyme electrode using the electro-synthesized PDA material. However, as far as we know, the investigation of the utilization of PD_M-Tyr modified electrode in environmental pollutants biosensing (phenol and related compounds, atrazine), which is meaningful both in environmental protection and in enzymology, has not been reported to date.

Herein, PD_M is catalytically synthesized by adding 8.5 mg mL^{-1} Tyr to 0.10 M PBS containing 10 mM L-DOPA and reacting in refrigerator (4 ^oC) for 2 h, with Tyr effectively entrapped in the prepared PD_M and thus PD_M-Tyr composite obtained. Tyr modified electrode is prepared by dipping a certain amount of resultant PD_M-Tyr composite on an Au electrode and then covered with Nafion. PD_M was used as an in situ Tyr-immobilization matrix for high performance amperometric biosensing of phenol compounds (phenol, *p*-chlorophenol, *o*-dihydroxybenzene, *p*-cresol) and atrazine. The PD_M is demonstrated to be effective in entrapping high-load and high activity Tyr, and the resultant enzyme electrodes prepared by casting the PD_M-Tyr composites on Au electrode exhibit excellent performance in phenol and related compounds sensing, which also serve well as novel atrazine biosensors.

2. Experimental

2.1. Instrumentation and Chemicals

All electrochemical experiments were conducted on a CHI660C electrochemical workstation (ChenHua Instruments Co., Shanghai, China) with a conventional three-electrode system. The Au disk electrode with 3.0 mm diameter served as the working electrode, a KCl-saturated calomel electrode (SCE) as the reference electrode, and a Pt wire as the counter electrode. All potentials reported here were cited versus SCE. UV-vis spectra were collected on a UV2450 UV-vis spectrophotometer (Shimadzu Co., Japan). Scanning electron micrographs (SEM) studies were performed on a Hitachi S4800 scanning electron microscope with a field emission electron gun.

Atomic force microscopy (AFM) images were collected on a PicoPlus atomic force microscope (Molecular Imaging Co., USA).

Tyr (EC 1.14.18.1; 4.80 kU mg^{-1} of solid, from mushroom) and atrazine was purchased from Sigma. L-DOPA, DA and Nafion (perfluoinated ion-exchange resin, 10 wt.% solution in water) were purchased from Aladdin. Phenol, *p*-chlorophenol, *o*-dihydroxybenzene, *p*-cresol and other chemicals were of analytical grade and purchased from Sinopharm Chemical Reagent Co., Ltd. (Shanghai, China). Phosphate buffer solution (PBS, pH 7.0) consisting of 0.10 M KH_2PO_4–K_2HPO_4 + 0.1 M K_2SO_4 served as the supporting electrolyte. Milli-Q ultrapure water (Millipore, ≥18 M) was used throughout. All experiments were performed at room temperature around 20 ^oC.

2.2. Procedures

Before modification, bare Au electrode was polished with 0.30 μm alumina powder and ultrasonic washed for at least 10 min in distilled water for three times. Then, the Au electrodes were treated with Piranha solution (H_2SO_4 : H_2O_2, 3:1 in *v*/*v*) for 15 s and dried under a nitrogen stream. Lastly, the electrochemical cleaning of Au electrode was carried out in sulfuric acid solution until repeated cyclic voltammograms obtained. The Au electrodes were then characterized by cyclic voltammetry in 2 mM $K_4Fe(CN)_6$ + 0.1 M K_2SO_4, and the peak-to-peak separation was observed to be within 75 mV, confirming that the Au electrode was well cleaned for subsequent experiments.

The construction procedure of Nafion/PD_M-Tyr/Au biosensor and its application in detection of phenol and atrazine is outlined in Scheme 1. A mildly stirred 0.10 M PBS containing 10.0 mM L-DOPA (I) was subject to enzyme catalytic polymerization with the addition of 8.5 mg mL^{-1} Tyr (I~II). It is visible that PD_M-Tyr precipitates were obtained immediately (II). The mixed solution was kept to react for 2 h to achieve reaction equilibrium, and then 5.0 μL of the prepared PD_M-Tyr suspension was cast on a clean Au electrode (Au, III), and 2.0 μL of 0.025 wt.% Nafion solution was immediately cast to strengthen the enzyme film (IV) and then air-dried. The thus

prepared enzyme electrode was used for phenol and atrazine biosensing in the following experiments. The freshly prepared enzyme electrode was water-rinsed and stored in PBS at 4 ^{o}C when not in use. For comparison, PD modified electrode prepared via electrochemical oxidation (PD_E electrode) was also fabricated by cyclic voltammetry (CV, here −0.50 ~ 0.50 V, 30.0 mVs^{-1}, 20 cycles) in unstirred PBS solution containing 10.0 mM L-DOPA. PD prepared via chemical oxidation (PD_C) was prepared by adding 5.0 mM $KMnO_4$ solution to a stirred 0.10 M PBS containing 10.0 mM L-DOPA and keeping reacting for 2 h.

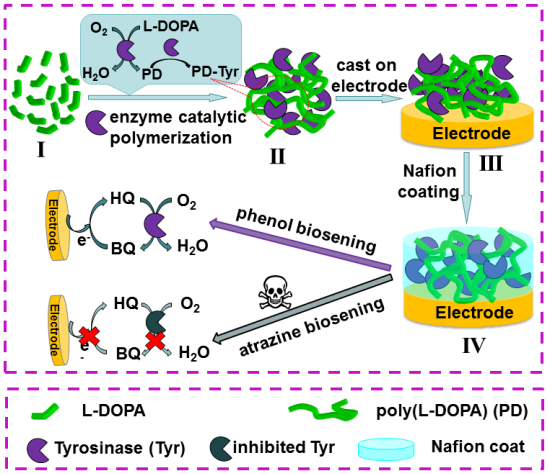

Scheme 1. Schematic representation of procedures for preparing Nafion/PD_M-Tyr/Au electrode and its application in detection of phenol and inhibitive-based detection of atrazine.

During phenol biosensing experiments, the steady-state current responses of the Tyr-based electrodes at various phenol concentrations were recorded at -0.20 V by successive injections of a certain concentrated phenol solution into 10 mL of stirred PBS (pH 7.0), and the electroreduction of the enzymatically generated *o*-benzoquinone (BQ) was detected. The response current was marked with the change value between the steady-state current and the background current (Δi).

In the inhibition biosensing, atrazine sensing was realized based on the inhibition effect of atrazine towards the catalytic activity of Tyr. At first, the signal of this sensor to the addition of 5.0 μM phenol solution was recorded as I_0. The biosensor was then incubated in atrazine-containing PBS solutions for 15 min, and the current response of the inhibited biosensor to 5.0 μM phenol solution was recorded as I_i, with the inhibition percentage (In(%) = (I_0 - I_i)/I_0)

used as the quantitative signal. After each inhibition measurement, the biosensor presented good operational stability and recoverability by incubation in PBS containing the substrate for at least 10 min (without chart).

UV-vis spectrophotometry was performed for investigating the enzyme-catalyzed oxidation of L-DOPA by Tyr and the UV-vis absorption spectra of 0.10 M PBS containing 0.5 mM L-DOPA, 50 μg mL^{-1} Tyr, or 0.5 mM L-DOPA + 50 μg mL^{-1} Tyr were taken and compared, with the time-dependent spectra during the Tyr-catalyzed oxidation of L-DOPA recorded. Fourier transform infrared (FTIR) spectra were collected on a Nicolet Nexus 670 FTIR instrument in the transmission mode. All FTIR spectra were collected at an average factor of 100 and a wave number resolution of 4 cm^{-1}.

3. Results and Discussion

3.1. Tyr-Catalyzed Polymerization of L-DOPA.

Tyr is used here to catalyze the polymerization of L-DOPA in aqueous solution. UV-vis spectroscopy was employed to monitor the enzyme-catalyzed oxidation of L-DOPA. As shown in Fig. 1(a, left), in a 0.10 M PBS (pH 7.0) containing 100 μM L-DOPA, an intense band was observed at 280 nm, which is directly related to the symmetry-forbidden transitions of the L-DOPA molecule. A broad band was observed at 280 nm for Tyr (inset of Fig. 1(left)), which can be related to the symmetry-forbidden transitions of aromatic amino acid residues[44]. The time-dependent spectra obtained during the Tyr-catalyzed oxidation of L-DOPA are shown in Fig. 1(b-e). During the oxidation, the band peaking at ~308 nm rose progressively in intensity and an intense band peaking at 480 nm rose, which is a characteristic electronic transition of the chrome form of the oxidized state of L-DOPA after intramolecular cyclization [44, 48]. Fig. 1(right) shows the FTIR spectra of L-DOPA and PDM formed by L-DOPA oxidation for comparison. Significant bands of 3500 ~ 3200 cm^{-1} in the spectrum of L-DOPA should be assigned to stretching or deformation vibrations of phenolic O–H bonds; and the long bands of 1500 ~ 600 cm^{-1} in L-DOPA spectra can also be attributed to significant bands of the phenolic O–H bonds,

which contains the surface deformation vibration peak and the out-of-plane deformation vibration peak of O–H bonds; bands around 1650 cm^{-1} in PD_M can be attributed to the stretching of aromatic C–C bonds and the C=O in newly formed benzoquinone; bands from 950 to 650 cm^{-1} are attributed to out-of-plane deformation of aromatic C–H bonds. Therefore, we may conclude that the polymer from L-DOPA enzyme oxidation can be most likely speculated as poly(5,6-indolequinone), and many oxygen atoms therein may have developed C–O–C chains during the poly(indole)-like polymerization [41]. This also demonstrated that L-DOPA was effectively oxidized under the function of Tyr.

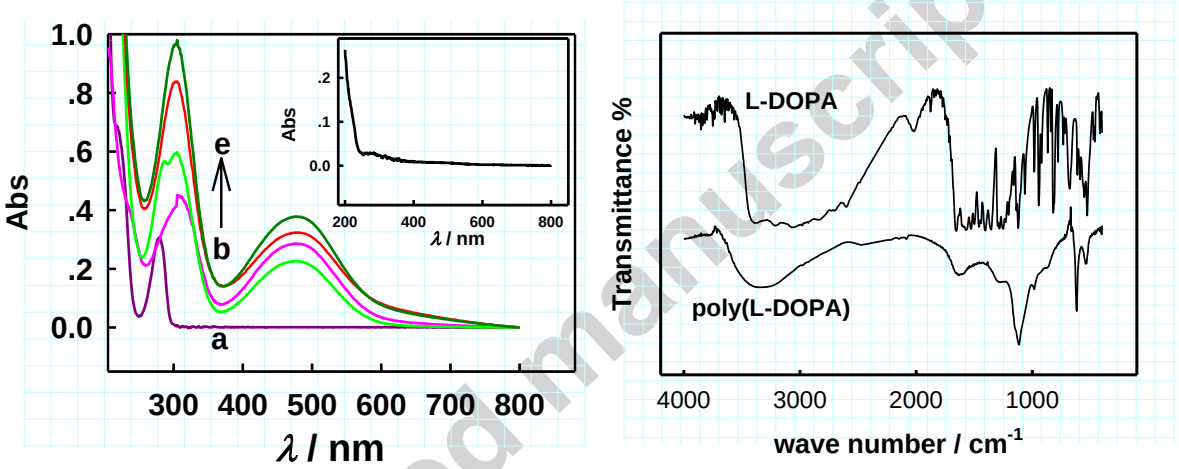

Fig. 1. UV-vis absorption spectra of 0.10 M PBS (pH 7.0) containing 0.5 mM L-DOPA (a) and 0.5 mM L-DOPA + 50 μg mL^{-1} Tyr (b-e, recorded every 3 min). Inset shows UV-vis absorption spectrum of 0.10 M PBS (pH 7.0) containing 50 μg mL^{-1} Tyr (Left). FT-IR spectra of L-DOPA and PD_M prepared under Tyr catalyzed oxidation (Right).

The SEM pictures and AFM images of PD modified electrode prepared via electrochemical oxidation (PD_E), chemical oxidation (PD_C) and enzyme oxidation (PD_M) were collected. As seen in Fig. 2, the PD_E/Au (A, a) shows a rather thin film, which is limited by the insulating nature of PD and is bad for entrapping large amounts of enzyme. With the coat of PD_C (B, b) or PD_M (C, c) on the Au disk electrode, we can clearly observe a relative thick blanket of biocomposites film. Comparing PD_C (B, b) with PD_M (C, c), we can find that the PD_M prepared under the oxidation function of Tyr was uniformly distributed, which may demonstrate enzyme oxidation is more effective in entrapping high load and high activity Tyr.

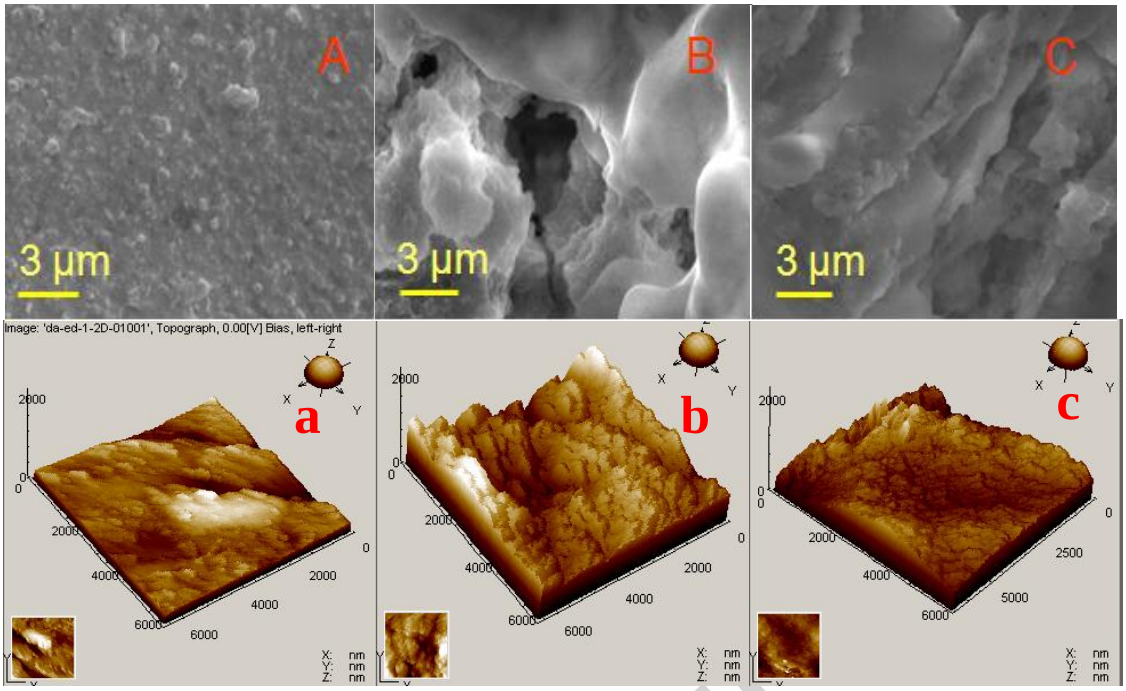

Fig. 2. SEM pictures of PD_E/Au (A), PD_C/Au (B), PD_M/Au (C) electrode surface and AFM images of PD_E/Au (a), PD_C/Au (b), PD_M/Au (c).

The electrochemical features of the Nafion/PD_M-Tyr/Au were also validated by electrochemical techniques. Fig. 3 (left panel) depicts the CV curves of Nafion/PD_M-Tyr/Au in 0.1 M PBS (pH 7.0) without (dotted and black line) and with increasing concentrations of phenol (soild and colourful lines). As seen in the figure, no signal was observed in the select potential windows in blank PBS solution, while the CV curves reflected obvious increases in reduction current with the additions of phenol. This current increase is due to the reduction of quinone species liberated from the enzyme reaction catalyzed by the Tyr on electrode surface [12]. The appearance of the reduction current indicates that the immobilization process retained the biological activity of Tyr. Under the catalysis of the Tyr on the electrode surface, phenol was oxidized by dissolving oxygen to form *o*-quinone and then reduced into catechol. We also investigated the relationship of current peak (i_p) with the square roots of sweep rate ($v^{1/2}$). As shown in Fig. 3(middle panel), the i_p is proportional to $v^{1/2}$, indicating that the electrochemistry of the produced BQ is a diffusion control process. The CVs of Nafion/PD_M-Tyr/Au obtained by multirun scanning (100 segments) in 0.1 M PBS containing 50.0 μM phenol was shown in Fig. 3(right

panel), we can see the prepared biosensor is relatively stable in phenol sensing. The slow decrease in the reduction peak current may be caused by poison of electrode by the product from enzymatic reaction.

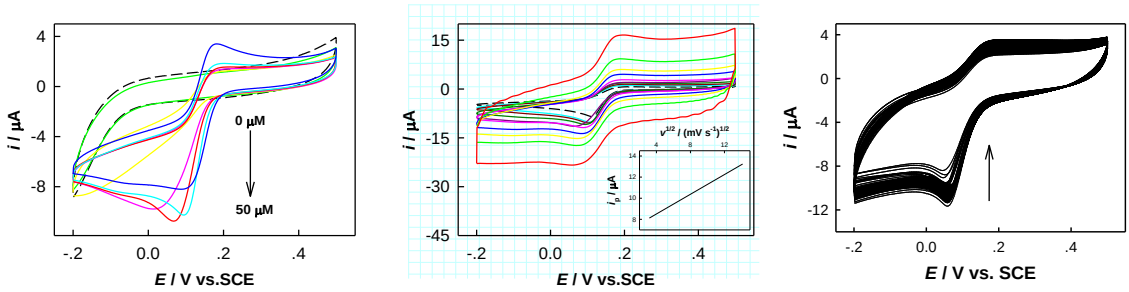

Fig. 3. CVs of Nafion/PD_M-Tyr/Au in 0.1 M PBS (pH 7.0) without (dotted and black) and with increasing concentrations of phenol (1.0 μM ~ 50.0 μM) (left), CVs at varying scan rates and the relationship of current peak (i_p) with the square roots of sweep rate ($v^{1/2}$) in 0.10 M PBS (middle), and the CVs of Nafion/PD_M-Tyr/Au obtained by multirun scanning (100 segments) in 0.1 M PBS containing 50.0 μM phenol (right).

3.2. Analytical performance of the Tyr biosensor

3.2.1. Optimization of experimental conditions.

To obtain the highest sensitivity for biosensing, various conditions, including the concentration of Tyr, the concentation of L-DOPA, the amount of Nafion, detection potentials and pH values, were optimized according to the biosensing signal output via variation of the examined one while others fixed, with the results shown in Table 1. We found that the biosensor gave maximum response at Tyr concentration of 8.5 mg mL^{-1}, L-DOPA concentration of 10 mM, and 2.0 μL 0.025 wt% Nafion. Such low concentration of Nafion was optimized and used here to ensure maintaining the enzymatic activity of Tyr, which was also demonstrated experimentally. The pH of PBS and the applied potential used for phenol and atrazine sensing was optimized, and pH 7.0 and an applied potential of -0.20 V vs. SCE (Quinones-reduction mode) with the maximum current response were selected as reported previously.

Table 1. Optimized conditions for enzyme electrode fabrication.

Experimental Parameters	Testing Range	Optimized Value
Tyrosinase concentration (mg mL^{-1})	1.0 ~ 15.0	8.5
L-DOPA concentration (mM)	5.0 ~ 25.0	10
Nafion (0.025 wt.%) volumn (μL)	0.5 ~ 3.0	2.0
Applied potentials (V, vs SCE)	-0.35 ~ 0	-0.20
pH of PBS solution	4.5 ~ 9.18	7.0

To test the performance of the constructed biosensors, the steady-state currents for enzyme electrodes under optimized conditions were examined in stirred PBS. Fig.4 illustrates the typical current-time plots of the sensor to the successive additions of phenolic compounds under optimized conditions. The biosensor responded rapidly to the additions of various substrates. The corresponding calibration curves of Nafion/PD_M-Tyr/Au to these substrates were shown in the insets in Fig.4. The biosensing performance of the resultant biosensor to phenol, *p*-chlorophenol, *p*-cresol and *o*-dihydroxybenzene were comparatively examined, with the sensitivity (*S*), limit of detection (LOD), and linear range (LR) presented in Table 2. Fast and sensitive response towards phenolic compounds reaches steady-state within 10 s, with the response time being ca. 6 s to phenols, ca. 8 s to *p*-chlorophenol, ca. 7 s to *p*-cresol, and ca. 9 s to *o*-dihydroxybenzene. As comparing with many reported results shown in Table 3, our Nafion/PD_M-Tyr/Au electrode exhibits the highest sensitivity and the lowest LOD to phenol and related compounds, which may result from the efficiency of the protocol of Tyr-catalytic polymerization L-DOPA in in-situ immobilizing high-load and high-activity Tyr. The high effective immobilization of Tyr was achieved through this self-catalytic polymerization and in-situ entrapping protocol and was expected to be able to find wider applications.

The apparent Michaelis-Menten constant (K_M^{app}) of the Nafion/PD_M-Tyr/Au, an indication of both the enzymatic affinity and the enzyme-substrate kinetic constants, is determined from the electrochemical Lineweaver-Burk form of the Michaelis-Menten equation. An electrochemical Lineweaver-Burk plot ($1/I$ versus $1/c_{phenol}$) leads to a straight line and provides values of K_M^{app}/I_{max} (slope) and $1/I_{max}$ (y-axis intercept) [24]. The K_M^{app} value displays the affinity of an enzyme for its substrate, and a lower K_M^{app} value indicates stronger substrate binding and higher catalytic activity. In the present study, K_M^{app} value is calculated to be 3.13 μM for the enzyme immobilized by taking the case in phenol sensing as an example (inset in panel A of Fig.4 and Table 2), which is obviously lower than the reported values, such as 24.7 μM for Tyr immobilized on vertical growth TiO_2 nanotubes, [24] 26.1 μM for Tyr entrapped in a vapor

deposited titania sol-gel membrane [5] and 721 μM of Tyr/gelatin modified GCE [50]. The low K_M^{app} value here indicates that the Tyr molecules entrapped in the enzyme-catalyzed formed PD_M retain their bioactivity and have high affinity for phenol, consequently, allowing higher sensitivity. This also demonstrated that Nafion/PD_M-Tyr/Au is an excellent biosensor.

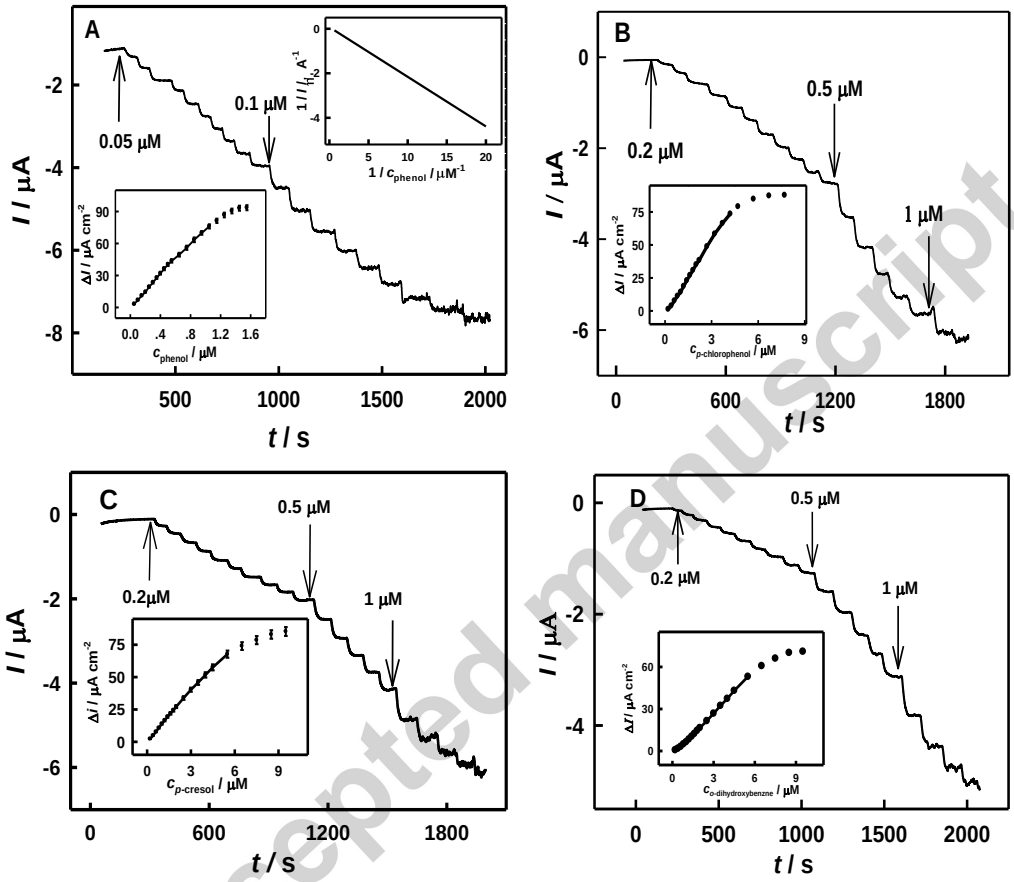

Fig. 4. Typical current-time curve of the enzyme electrode for phenols (A), *p*-chlorophenol (B), *p*-cresol (C), and *o*-dihydroxybenzene (D) in 0.10 mol L^{-1} PBS (pH 7.0) at -0.20 V. Insets: relationship between the catalytic current and the concentration of phenolics for Nafion/PD_M-Tyr/Au electrode.

Table 2. Analytical performances of biosensor

Detection substrate	Sensitivity ($\mu A\ mM^{-1}$)	Detection limit (μM)	Liner range (μM)	K_M^{app} (μM)
phenol	5122	0.002	0.01~ 1.25	3.13
p-chlorophenol	1293	0.03	0.1~ 4.2	3.36
p-cresol	926	0.02	0.1~5.6	14.80
o-dihydroxybenzene	728	0.05	0.1~ 6.4	3.69

Table 3. Comparison of performances of Nafion/PD_M-Tyr/Au for phenol sensing.

Immobilization method	LOD (μM)	Sensitivity (μA mM^{-1})	Liner Range (mM)
Tyr-titania sol-gel films[12]	10	103	_
Tyr-silica sol film[22]	0.1	23.1	_
Tyr/silicate/Nafion[7]	10	46	_
Tyr-AuNPs-graphite–Teflon composite[9]	0.06	746	4.0×10^{-4} ~ 7.0×10^{-2}
Tyr-copolymerpoly(N-3-aminopropyl pyrrole-co-pyrrole) film[6]	1.2	3.46	1.6×10^{-2} ~ 0.12
Tyr-MWCNTs-Nafion nanobiocomposite matrix[4]	0.22	346	1.0×10^{-3} ~ 2.3×10^{-2}
Tyr/agarose-guargum[10]	6.0	_	6.0×10^{-5} ~ 8.0×10^{-4}
Tyr-1,6-hexanedithiol and nano-Au self-assembled monolayers[26]	0.06	3.94	4.0×10^{-4} ~ 7.0×10^{-2}
∗This artical	0.002	5122	1.0×10^{-5} ~1.25×10^{-3}

3.2.2. The inhibitive sensing of atrazine

As an important part in melanin synthesis, the inhibition of Tyr could efficiently delay the procedure of enzymatic browning. Now Tyr inhibitors were widely used in food antibrowning and skin hyperpigmentation treatment. A Tyr-immobilized biosensor can be used for the high sensitive atrazine biosensing based on the fact that atrazine inhibits the catalytic activity of Tyr to phenols. Detection of atrazine by inhibition of Tyr has been widely reported [23-24]. Experimentally, we immersed the fabricated biosensor in PBS solutions and the signal of this sensor to the addition of 5.0 μM phenol solution was recorded as I_0. The biosensor was then incubated in atrazine-containing PBS solutions for 15 min, then the signal of the inhibited biosensor to 5.0 μM phenol solution was recorded as I_i, with the inhibition percent (In(%)) recorded as In(%) = (I_0 - I_i)/I_0. After each inhibition measurement, the biosensor presented good operational stability and recoverability in 10 min by incubation in PBS containing the substrate (without chart). Fig. 5 shows that In(%) increases with pesticide concentration, and the largest inhibition percent is more than 80%. A detection limit of 10 ppb (based on a signal-to-noise ratio of 3) was obtained. A linear calibration curve could be obtained in the range of 50 ppb ~ 3.0 ppm of atrazine by using a reciprocal plot. The limit of detection obtained in this work is lower than that obtained on Tyr-screen printed electrodes (0.3 ppm) [51], Tyr-controlled porosity glass (0.5 ppm) [52], Tyr-Au electrode (1.08 ppm) [23] and cationic amphiphilic pyrrole-Tyr electrode (0.86 ppm)

[53]. Thus, a novel atrazine biosensor with excellent bioelectrochemical interface is successfully prepared, which also presents high sensitivity and low detection limit.

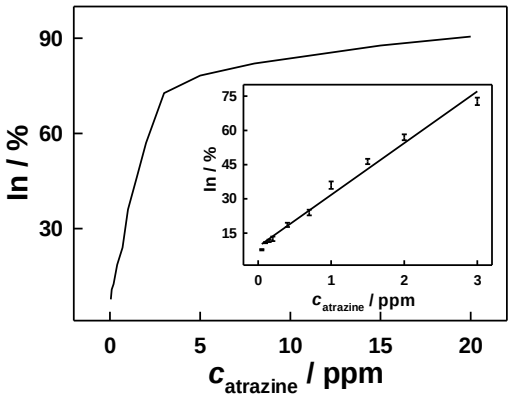

Fig. 5. The inhibition curves of Nafion/PD_M-Tyr/Au for atrazine in 0.1 M PBS (pH 7.0) at -0.20 V. Insert: calibration curve for atrazine.

3.2.3. Stability and Repeatability

The long term stability and repeatability of the sensor to phenol and atrazine sensing was tested. The long term stability to phenol sensing was evaluated by monitoring the amperometric responses to additions of 0.2 μM phenol at 2 day intervals over a period of 4 weeks, with the results shown in Fig. 6(A). The biosensor maintains 90% of the initial response in the first week and then decreased gradually to 78% after 4 weeks. The performance of the Nafion/PD_M-Tyr/Au electrode to atrazine sensing changes little with the incubation time. These results demonstrate that this biosensor has excellent long term stability. The repeatability of the Nafion/PD_M-Tyr/Au electrode was evaluated for six identical electrodes prepared independently on different days but following the same electrode construction protocol. The average steady-state current after addition of 0.2 μM phenol shows a relative standard deviation of 1.2%. The repeatability to atrazine sensing is examined experimentally and the inhibition percent (In(%)) of the biosensor changed little with the repeated determinations.

The amperometric responses of the prepared biosensor to some potential interferences (Mg^{2+}, Ca^{2+}, Cu^{2+}, Ag^{+}, SO_4^{2-}, HCO_3^{-}, and Cl^{-}), which are usually met in waters, were investigated to study its anti-interference ability[54]. As shown in Fig. 6(B), for the measurement of 0.4 μM

phenol, 0.10 mM Mg^{2+}, Ca^{2+}, Cu^{2+}, Ag^{+}, SO_4^{2-}, HCO_3^{-}, and Cl^{-} have no interference. This means that the biosensor exhibits excellent anti-interference ability and have potential applications in the determination of phenolic compounds in real water samples.

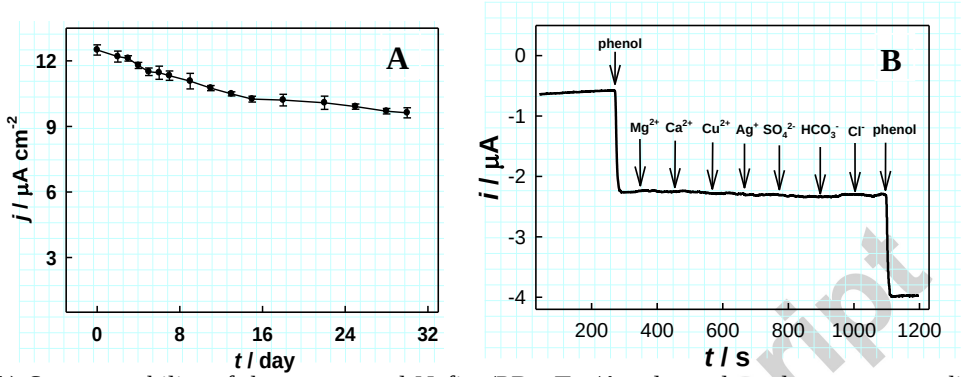

Fig. 6. (A) Storage stability of the constrccted Nafion/PD_M-Tyr/Au electrode under storage conditions (in 0.10 M PBS solution of pH 7.0 at 4 °C). (B) Current responses at the Nafion/PD_M-Tyr/Au electrode to the sequential additions of 0.4 μM phenol, 0.10 mM Mg^{2+}, Ca^{2+}, Cu^{2+}, Ag^{+}, SO_4^{2-}, HCO_3^{-}, Cl^{-} and 0.4 μM phenol into 0.10 M PBS aqueous solution (pH 7.0). The measurements were conducted at -0.20 V vs.SCE.

Table 4. Determination of phenolic compounds and atrazine in real water samples (n = 5) [a]

Sample	phenol				atrazine			
	Determined (nM)	Added (nM)	Found (nM)	Recovery (%)	Determined (ppb)	Added (ppb)	Found (ppb)	Recovery (%)
River water	18.2 ± 0.4	50.0	49.2 ± 1.4	98.4 ± 2.8	–	500	476 ± 11	95.2 ± 2.2
Lake water	10.1 ± 0.2	50.0	51.3 ± 1.6	102.6 ± 3.2	–	500	512 ± 16	102.4 ± 3.2
Farmland water	30.2 ± 0.5	50.0	50.6 ± 2.1	101.2 ± 4.2	115 ± 5	500	511 ± 20	102.2 ± 4.0

[a]All water samples were filtered with a 0.22 μm membrane (purchased from Millipore) in advance, 0.10 M K_2HPO_4–KH_2PO_4 + 0.10 M K_2SO_4 (final concentration, pH 7.0) were then added, and the samples were 10-fold diluted for determination.

To further study the practical performance of the proposed method, the biosensor was employed to determine trace amounts of phenolic compounds and atrazine in spiked water samples. For the analysis, samples from Xiangjiang River (sample 1), Peach Lake (sample 2) and farmland waste water (sample 3) in Changsha, Hunan Province (China), were filtered, then spiked with various concentrations of phenol or atrazine and analyzed according to the procedure described in the footnote in Table 4. Each sample was analyzed five times. The recoveries were in the range of 95.6 to 105.8% in phenol determination and in the range of 93.0% to 106.2% in atrazine sensing, indicating good accuracy and validating the potential utility of the present biosensor for total phenol compounds and atrazine detection in natural water samples.

4. Conclusions

In this work, taking L-DOPA as the monomer and Tyr as the enzyme catalyst for L-DOPA polymerization, we synthesized the PD_M-Tyr composites and realized the sensitive phenols and atrazine sensing by constructing a biosensor via immobilizing Tyr with enzyme-catalyzed fabricated PD_M. The preliminarily practical application in the determination of phenolic compounds and atrazine in river water, lake water and farmland waste water exhibited satisfying results. The resultant biosensor displayrd high sensitivity, selectivity, stability, and fabrication simplicity, which can be used for the accurate determination of several phenolic compounds or some inhibitors and there will be a broad space for development in the future.

Acknowledgments

This work was supported by the National Natural Science Foundation of China (21405042, 21475041, 21175042, 21305041), the Open Fund of State Key Laboratory of Chemo/Biosensing and Chemometrics (Hunan University) and A Project Supported by Scientific Research Fund of Hunan Provincial Education Department.

References

[1] A. Karioti; A. Protopappa; N. Megoulas; H. Skaltsa, Identification of tyrosinase inhibitors from Marrubium velutinum and Marrubium cylleneum. Bioorg. Med. Chem. 15 (2007) 2708-2714.

[2] H. S. Mason, The chemistry of melanin; mechanism of the oxidation of dihydroxyphenylalanine by tyrosinase. J Biol. Chem. 172 (1948) 83-99.

[3] H. B. Yildiz; R. Freeman; R. Gill; I. Willner, Electrochemical, photoelectrochemical, and piezoelectric analysis of tyrosinase activity by functionalized nanoparticles. Anal. Chem. 80 (2008) 2811-2816.

[4] Y. C. Tsai; C. C. Chiu, Amperometric biosensors based on multiwalled carbon nanotube-Nafion-tyrosinase nanobiocomposites for the determination of phenolic compounds. Sens. Actuators, B 125 (2007) 10-16.

[5] S. Campuzano; B. Serra; M. Pedrero; F. J. M. Villena; J. M. Pingarron, Amperometric flow-injection determination of phenolic compounds at self-assembled monolayer-based tyrosinase biosensors. Anal. Chim. Acta 494 (2003) 187–197.

[6] Rajesh; W. Takashima; K. Kaneto, Amperometric phenol biosensor based on covalent immobilization of tyrosinase onto an electrochemically prepared novel copolymer poly (N-3-aminopropyl pyrrole-co-pyrrole) film. Sens. Actuators, B 102 (2004) 271-277.

[7] M. A. Kim; W.-Y. Lee, Amperometric phenol biosensor based on sol–gel silicate/Nafion composite film. Anal. Chim. Acta 479 (2003) 143-150.

[8] Rajesh; W. Takashima; K. Kaneto, Amperometric tyrosinase based biosensor using an electropolymerized PTS-doped polypyrrole film as an entrapment support. React. Funct. Polym. 59 (2004) 163-169.

[9] V. Carralero; M. L. Mena; A. Gonzalez-Cortés; P. Yáñez-Sedeño; J. M. Pingarrón, Development of a high analytical performance-tyrosinase biosensor based on a composite graphite–Teflon electrode modified with gold nanoparticles. Biosens. Bioelectron. 22 (2006) 730-736.

[10] S. Tembe; S. Inamdar; S. Haram; M. Karve; S. F. D'Souza, Electrochemical biosensor for catechol using agarose-guar gum entrapped tyrosinase. J Biotechnol. 128 (2007) 80-85.

[11] Y. C. Fu; P. H. Li; L. J. Bu; T. Wang; Q. J. Xie; J. H. Chen; S. Z. Yao, Exploiting metal-organic coordination polymers as highly efficient immobilization matrixes of enzymes for sensitive electrochemical biosensing. Anal. Chem. 83 (2011) 6511-6517,.

[12] J. Yu; S. Liu; H. Ju, Mediator-free phenol sensor based on titania sol–gel encapsulation matrix for immobilization of tyrosinase by a vapor deposition method. Biosens. Bioelectron. 19 (2003) 509-514.

[13] K. Maeda; M. Fukuda, In vitro effectiveness of several whitening cosmetic components in human melanocytes. J. Soc. Cosmet. Chem. 42 (1991) 361-368.

[14] J. Švitel; S. Miertuš, Development of tyrosinase-based biosensor and its application for monitoring of bioremediation of phenol and phenolic compounds. Environ. Sci. Technol. 32 (1998) 828-832.

[15] J. R. Rohr; A. M. Schotthoefer; T. R. Raffel; H. J. Carrick; N. Halstead; J. T. Hoverman; C. M. Johnson; L. B. Johnson; C. Lieske; M. D. Piwoni, Agrochemicals increase trematode infections in a declining amphibian species. Nature 455 (2008) 1235-1239.

[16] N. Graziano; M. J. McGuire; A. Roberson; C. Adams; H. Jiang; N. Blute, 2004 National atrazine occurrence monitoring program using the Abraxis ELISA method. Environ. Sci. Technol. 40 (2006) 1163–1171.

[17] J. Rayner; R. Enoch; S. Fenton, Adverse effects of prenatal exposure to atrazine during a critical period of mammary gland growth. Toxicol. Sci. 87 (2005) 255-266.

[18] E. Silva; A. M. Fialho; I. Sa-Correia; R. G. Burns; L. J. Shaw, Combined bioaugmentation and biostimulation to cleanup soil contaminated with high concentrations of atrazine. Environ. Sci. Technol. 38 (2004) 632–637.

[19] W. T. Ma; K. K. Fu; Z. W. Cai; G. B. Jiang, Gas chromatography/mass spectrometry applied for the analysis of triazine herbicides in environmental waters. Chemosphere 52 (2003) 1627–1632.

[20] C. D. Chriswell; R. C. Chang; J. S. Fritz, Chromatographic determination of phenols in water. Anal. Chem. 47 (1975) 1325-1329.

[21] P. Panuwet; J. V. Nguyen; P. Kuklenyik; S. O. Udunka; L. L. Needham; D. B. Barr, Quantification of atrazine and its metabolites in urine by on-line solid-phase extraction-highperformance liquid chromatography-tandem mass spectrometry. Anal. Bioanal. Chem. 391 (2008) 1931–1939.

[22] B. Wang; J. Zhang; S. Dong, Silica sol–gel composite film as an encapsulation matrix for the construction of an amperometric tyrosinase-based biosensor. Biosens. Bioelectron. 15 (2000) 397-402.

[23] F. A. McArdle; K. C. Persaud, Development of an enzyme-based biosensor for atrazine detection. Analyst 118 (1993) 419-423.

[24] Z. Yu; G. Zhao; M. Liu; Y. Lei; M. Li, Fabrication of a novel atrazine biosensor and its subpart-per-trillion levels sensitive performance. Environ. Sci. Technol. 44 (2010) 7878–7883.

[25] Y. Fu; C. Zou; L. Bu; Q. Xie; S. Yao, Novel amperometric aptasensor based on analyte-induced suppression of enzyme catalysis in polymeric bionanocomposites. ACS Appl. Mater. Interfaces 5 (2013) 934-939.

[26] Z. Liu; J. Liu; G. Shen; R. Yu, A reagentless tyrosinase biosensor based on 1,6-hexanedithiol and nano-Au self-assembled monolayers. Electroanalysis 18 (2006) 1572-1577.

[27] A. A. Karyakin; E. A. Kotel'nikova; L. V. Lukachova; E. E. Karyakina; J. Wang, Optimal environment for glucose oxidase in perfluorosulfonated Ionomer membranes: improvement of first-generation biosensors. Anal. Chem. 74 (2002) 1597-1603.

[28] Y. Liu; K. Ai; L. Lu, Polydopamine and its derivative materials: synthesis and promising applications in energy, environmental, and biomedical fields. Chem. Rev. 114 (2014) 5057-5115.

[29] J. T. Arena; B. McCloskey; B. D. Freeman; J. R. McCutcheon, Surface modification of thin film composite membrane support layers with polydopamine: Enabling use of reverse osmosis membranes in pressure retarded osmosis. J. Membr. Sci. 375 (2011) 55-62.

[30] C. Cheng; S. Li; W. Zhao; Q. Wei; S. Nie; S. Sun; C. Zhao, The hydrodynamic permeability and surface property of polyethersulfone ultrafiltration membranes with mussel-inspired polydopamine coatings. J. Membr. Sci. 417–418 (2012) 228-236.

[31] B. D. McCloskey; H. B. Park; H. Ju; B. W. Rowe; D. J. Miller; B. D. Freeman, A bioinspired fouling-resistant surface modification for water purification membranes. J. Membr. Sci. 413–414 (2012) 82-90.

[32] S. Kasemset; A. Lee; D. J. Miller; B. D. Freeman; M. M. Sharma, Effect of polydopamine deposition conditions on fouling resistance, physical properties, and permeation properties of reverse osmosis membranes in oil/water separation. J. Membr. Sci. 425–426 (2013) 208-216.

[33] Y. Li; Y. Su; X. Zhao; X. He; R. Zhang; J. Zhao; X. Fan; Z. Jiang, Antifouling, high-flux nanofiltration membranes enabled by dual functional polydopamine. ACS Appl. Mater. Interfaces 6 (2014) 5548-5557.

[34] H. C. Yang; J. K. Pi; K. J. Liao; H. Huang; Q. Y. Wu; X. J. Huang; Z. K. Xu, Silica-decorated polypropylene microfiltration membranes with a mussel-inspired intermediate layer for oil-in-water emulsion separation. ACS Appl. Mater. Interfaces 6 (2014) 12566-12572.

[35] L. Huang; J. T. Arena; S. S. Manickam; X. Jiang; B. G. Willis; J. R. McCutcheon, Improved mechanical properties and hydrophilicity of electrospun nanofiber membranes for filtration applications by dopamine modification. J. Membr. Sci. 460 (2014) 241-249.

[36] X. Wang; Z. Jiang; J. Shi; C. Zhang; W. Zhang; H. Wu, Dopamine-modified alginate beads reinforced by cross-linking via titanium coordination or self-polymerization and its application in enzyme immobilization. Ind. Eng. Chem. Res. 52 (2013) 14828-14836.

[37] L. Zhang; J. Shi; Z. Jiang; Y. Jiang; S. Qiao; J. Li; R. Wang; R. Meng; Y. Zhu; Y. Zheng, Bioinspired preparation of polydopamine microcapsule for multienzyme system construction. Green Chem. 13 (2011) 300-306.

[38] H. Lee; J. Rho; P. B. Messersmith, Facile conjugation of biomolecules onto surfaces via mussel adhesive protein inspired coatings. Adv. Mater. 21 (2009) 431-434.

[39] D. Li; L. Luo; Z. Pang; L. Ding; Q. Wang; H. Ke; F. Huang; Q. Wei, Novel phenolic biosensor based on a magnetic polydopamine-Laccase-nickel nanoparticle loaded carbon nanofiber composit. ACS Appl. Mater. Interfaces 6 (2014) 5144-5151.

[40] C. Chao; J. Liu; J. Wang; Y. Zhang; B. Zhang; Y. Zhang; X. Xiang; R. Chen, Surface Modification of Halloysite Nanotubes with Dopamine for Enzyme Immobilization. ACS Appl. Mater. Interfaces. 5 (2013) 10559–10564.

[41] Y. Li; M. Liu; C. Xiang; Q. Xie; S. Yao, Electrochemical quartz crystal microbalance study on growth and property of the polymer deposit at gold electrodes during oxidation of dopamine in aqueous solutions. Thin Solid Films 497 (2006) 270-278.

[42] H. Lee; S. M. Dellatore; W. M. Miller; P. B. Messersmith, Mussel-inspired surface chemistry for multifunctional coatings. Science 318 (2007) 426-430.

[43] Y. Fu; P. Li; Q. Xie; X. Xu; L. Lei; C. Chen; C. Zou; W. Deng; S. Yao, One-pot preparation of polymer–enzyme–metallic nanoparticle composite films for high-performance biosensing of glucose and galactose. Adv. Funct. Mater. 19 (2009) 1784-1791.

[44] Y. Tan; W. Deng; Y. Li; Z. Huang; Y. Meng; Q. Xie; M. Ma; S. Yao, Polymeric bionanocomposite cast thin films with in situ Laccase-catalyzed polymerization of dopamine for biosensing and biofuel cell applications. J. Phys. Chem. B 114 (2010) 5016-5024.

[45] J. H. Waite; M. L. Tanzer, The bioadhesive of Mytilus byssus: A protein containing L-DOPA. Biochem. Biophys. Res. Commun. 96 (1980) 1554-1561.

[46] J. H. Waite; M. L. Tanzer, Polyphenolic substance of mytilus edulis: novel adhesive containing L-DOPA and hydroxyproline. Science 212 (1981) 1038-1040.

[47] M. Dai; L. Sun; L. Chao; Y. Tan; Y. Fu; C. Chen; Q. Xie, Immobilization of enzymes by electrochemical and chemical oxidative polymerization of L-DOPA to fabricate amperometric biosensors and bofuel cells. ACS Appl. Mater. Interfaces 7 (2015) 10843-10852.

[48] M. Dai; T. Huang; L. Chao; Y. Tan; C. Chen*; W. Meng; Q. Xie*, Tyrosinase-catalyzed polymerization of L-DOPA (versus L-tyrosine and dopamine) to generate melanin-like biomaterials for immobilization of enzymes and amperometric biosensing. RSC Adv. 6 (2016) 17016-17022.

[49] M. Dai; T. Huang; L. Chao; Q. Xie; YuemingTan; C. Chen; W. Meng, Horseradish peroxidase-catalyzed polymerization of L-DOPA for mono-/bi-enzyme immobilization and amperometric biosensing of H2O2 and uricacid. Talanta 149 (2016) 117–123.

[50] N. Li; M. H. Xue; H. Yao; J. J. Zhu, Reagentless biosensor for phenolic compounds based on tyrosinase entrapped within gelatine film. Anal. Bioanal. Chem. 383 (2005) 1127–1132.

[51] C. Tortolini; P. Bollella; R. Antiochia; G. Favero; F. Mazzei, Inhibition-based biosensor for atrazine detection. Sens. Actuators, B 224 (2016) 552-558.

[52] A. Hipólito-Moreno; M. E. León-González; L. V. Pérez-Arribas; L. M. Polo-Díez, Non-aqueous flow-injection determination of atrazine by inhibition of immobilized tyrosinase. Anal. Chim. Acta 362 (1998) 187-192.

[53] J.-L. Besombes; S. Cosnier; P. Labbé; G. Reverdy, A biosensor as warning device for the detection of cyanide, chlorophenols, atrazine and carbamate pesticides. Anal. Chim. Acta 311 (1995) 255-263.

[54] J. Adamski; P. Nowak; J. Kochana, Simple sensor for the determination of phenol and its derivatives in water based on enzyme tyrosinase. Electrochim. Acta 55 (2010) 2363–2367.

Highlights

(1) Effective immobilization of Tyrosinase (Tyr) via enzyme catalytic polymerization of L-DOPA

(2) The thus-prepared Tyr immobilized electrode exhibits excellent performance superior to most previous reported values.

(3) The sensitivity to phenol increases by 1~4 orders of magnitude comparing with reported values, the biosensor also works well in atrazine biosensing.

(4) The proposed biosensor works well in real water samples determination

Graphical Abstract

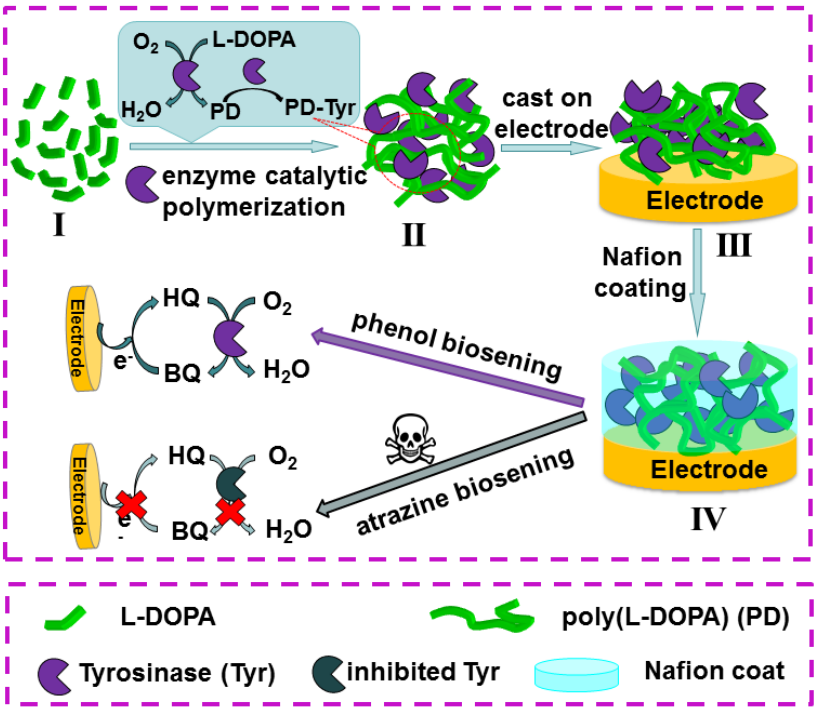

Scheme 1. Schematic representation of procedures for preparing Nafion/PD_M-Tyr/Au electrode and its application in detection of phenol and inhibitive-based detection of atrazine.